

Fractional revivals of superposed coherent states

M. Rohith¹, C. Sudheesh¹

¹ Department of Physics, Indian Institute of Space Science and Technology,
Thiruvananthapuram 695 547, India

Abstract. We study the dynamics of superposed wave packets in a specific nonlinear Hamiltonian which models the wave packet propagation in Kerr-like media and the dynamics of Bose-Einstein condensates. We show the dependence of initial wave packet superposition on fractional revival times using analysis based on the expectation values, Rényi entropy and Wigner function. We also show how the selective identification of fractional revivals using moments of appropriate observables depends on the number of wave packets present in the initial state.

PACS numbers: 42.50.-p, 03.67.-a

1. Introduction

Dynamics of the wave packet in a nonlinear media exhibits revivals and fractional revivals at specific instants of time, arising from the interference between the stationary states comprising the wave packet. The revival phenomena has been investigated both theoretically and experimentally in a wide class of systems [1]. An initial well localized quantum state spreads during the propagation and after certain time T_{rev} , the revival time, the wave packet localizes again giving rise to quantum wave packet revival. Fractional revival occurs when the initial wave packet evolves into a state that can be described as a collection of mini packets, each of which closely resembles the initial wave packet [2]. The fractional revival phenomena has been observed experimentally in a variety of quantum systems such as Rydberg atomic wave packets [3], molecular vibrational states [4], Bose-Einstein condensates [5], etc. Wave packet isotope separation is closely related to the revivals and fractional revivals, which provides the means of suppression of unwanted dispersion of wave packets [6]. The collapse and revival oscillations of first-order coherence were shown to be a sensitive measure of the nearest-neighbor couplings in the extended Bose-Hubbard model [7].

An initial wave packet $|\psi(0)\rangle$ spreads rapidly during the evolution governed by a nonlinear Hamiltonian and revivals are signaled by the return of the autocorrelation function $A(t) = |\langle\psi(0)|\psi(t)\rangle|^2$ to its initial value of unity. There are various methods in literature to identify and analyze fractional revivals. The distinctive signatures of the different fractional revivals of a suitably prepared initial wave packet are displayed in the mean values and higher moments of appropriate observables [8]. Entropy associated with phase distribution [9] or Rényi entropy [10] (sum of entropies associated with position and momentum space probability distributions) is also can be used to study the formation of macroscopic quantum superposition states. Wigner function plots can be used to visualize the revivals and fractional revivals in phase space.

The universal scenario of revivals described in [2] applies to an arbitrary initial superposition states, including a superposition of several wave packets as well. However, the generic analytical expressions of [2] and the revival phenomena discussed in a wide class of systems [1] are mainly dealing with the arbitrary initial superposition states. To date, revival phenomena of *superposed initial wave packets* received less attention in the literature. Thus, a problem of considerable interest is to study in detail the revivals and fractional revivals of initial superposed wave packets. For this purpose we use the example of a specific nonlinear Hamiltonian that is physically relevant in at least two important contexts: wave packet propagation in Kerr-like media [11,12], and the dynamics of BECs [5]. Generation of discrete superposition of coherent states at fractional revival times in the process of wave packet propagation in Kerr-like media is discussed in [13–15].

In most of the earlier studies [5,11–15], the initial state considered is an initial initial coherent state $|\psi(0)\rangle = |\alpha\rangle$, where $\alpha = |\alpha|e^{i\theta}$ is a complex number. The coherent state $|\alpha\rangle$ is defined as the eigenstate of the annihilation operator a , and its Fock state

representation is

$$|\alpha\rangle = e^{-|\alpha|^2/2} \sum_{n=0}^{\infty} \frac{\alpha^n}{\sqrt{n!}} |n\rangle. \quad (1)$$

For ready reference, in section 2 we review some of the relevant results pertained to revival and fractional revival of initial coherent state in the Kerr-like medium. In section 2 we also discuss how the fractional revivals are identified using expectation values [8], Wigner function and Rényi entropy [10].

Though the results obtained in [8, 13–15] are for an initial coherent state, they are applicable to any initial wave packet of the form

$$|\psi(0)\rangle = \sum_{n=0}^{\infty} C_n |n\rangle. \quad (2)$$

Another example for an initial state of the form given in equation (2) is m-photon-added coherent state [16]. Time evolution of initial m-photon-added coherent state in Kerr-like media shows revival and fraction revivals at same instants as in the case of initial coherent state [17].

This paper will discuss the fractional revivals of states where only every second, third, fourth, etc., expansion coefficient C_n differs from zero, and these states have not been looked at in detail in [8, 13–15, 17] before. Such states can be obtained by superposing l coherent states

$$|\psi_{l,h}\rangle = N_{l,h} \sum_{r=0}^{l-1} e^{-i2\pi r h/l} |\alpha e^{i2\pi r/l}\rangle, \quad (3)$$

where $h = 0, 1, 2, \dots, l-1$ and $N_{l,h}$ is a appropriate normalization constant. The number state representation of the state $|\psi_{l,h}\rangle$ is

$$|\psi_{l,h}\rangle = l N_{l,h} e^{-|\alpha|^2/2} \sum_{n=0}^{\infty} \frac{\alpha^{ln+h}}{\sqrt{(ln+h)!}} |ln+h\rangle, \quad (4)$$

which consists in an arithmetic infinite progression having the state $|h\rangle$ as initial term and a common difference, equal to l , between successive terms. The state $|\psi_{l,h}\rangle$ for a given l and h is also an eigenstate of the operator a^l with eigenvalue α^l [18]. If we set $l = 1$ and $h = 0$ in the above equation we retrieve the initial coherent state given in equation (1). For $l = 2$, we get two states which correspond to $h = 0$ and $h = 1$ and they are called even and odd coherent states respectively. In this paper we study in detail the initial states $|\psi_{l,h}\rangle$ with $h = 0$, denoted by

$$|\psi_l\rangle = N_l \sum_{r=0}^{l-1} |\alpha e^{i2\pi r/l}\rangle. \quad (5)$$

The state $|\psi_l\rangle$ is termed as *even coherent state of order l* [18] and its number state representation is

$$|\psi_l\rangle = l N_l e^{-|\alpha|^2/2} \sum_{n=0}^{\infty} \frac{\alpha^{ln}}{\sqrt{(ln)!}} |ln\rangle. \quad (6)$$

In sections 3 we study the dynamics of initial state $|\psi_2\rangle$ ($l = 2$), which is a superposition of two coherent states. We use the methods described in section 2 to study the effect of superposition of two coherent states on the revival and fractional revivals. In section 4 we extend our analysis to the superposition of three coherent states, i.e., $l = 3$ case in equation (5). In section 5 we generalize the results obtained in sections 3 and 4 to an arbitrary choice of initial superposed wave packets, $|\psi_l\rangle$, and discuss the possibility of experimental manifestations of our results.

2. Wave packet dynamics of coherent state in Kerr-like medium

The effective Hamiltonian for the propagation of coherent field in a Kerr medium [11, 12] is

$$H = \hbar\chi a^{\dagger 2} a^2 = \hbar\chi N(N-1) \quad (7)$$

with $N = a^{\dagger}a$, where a and a^{\dagger} are the usual photon annihilation and creation operator respectively and χ is a positive constant. The eigenstates of the operator N are the usual Fock basis $|n\rangle$. The numerical value of χ merely sets the time scale.

Consider the evolution of an initial coherent state $|\alpha\rangle$ through the medium. Such an initial state can be shown to revive periodically with revival time $T_{\text{rev}} = \pi/\chi$. Let $\alpha = \nu^{1/2} \exp(i\theta)$, where $\nu = |\alpha|^2$ is the mean number of photons in the coherent state. Without loss of generality, we set $\theta = \pi/4$ throughout this paper. In between $t = 0$ and $t = T_{\text{rev}}$, k-sub-packet fractional revivals occur for the initial wave packet at time $t = \pi j/k\chi$, where $j = 1, 2, \dots, (k-1)$ for a given value of $k(> 1)$ with a condition that j and k are mutually prime integers. Here onwards we use the notation $(r, s) = 1$ to denote the two mutually prime integers r and s . At fractional revival time $t/T_{\text{rev}} = j/k$, the initial wave packet splits into k sub-packets which resembles the initial wave packet. Thus, at k-sub-packet fractional revival times discrete superposition of k coherent states are generated [13–15]. For example, at $t = T_{\text{rev}}/4$

$$|\psi(t = T_{\text{rev}}/4)\rangle = \frac{1}{\sqrt{8}} \left[(1-i) |\alpha e^{i\pi/4}\rangle + \sqrt{2} |\alpha e^{-i\pi/4}\rangle - (1-i) |\alpha e^{-i3\pi/4}\rangle + \sqrt{2} |\alpha e^{i3\pi/4}\rangle \right], \quad (8)$$

which is a superposition of four coherent states.

Consider the operators

$$x = \frac{(a + a^{\dagger})}{\sqrt{2}} \quad \text{and} \quad p = \frac{(a - a^{\dagger})}{i\sqrt{2}}. \quad (9)$$

It is convenient to introduce the notation

$$\alpha = \alpha_1 + i\alpha_2 = \frac{(x_0 + ip_0)}{\sqrt{2}},$$

where x_0 and p_0 represent the locations of the centers of the Gaussian wave packets corresponding to the coherent state $|\alpha\rangle$. For $\nu = 20$, (x_0, p_0) for the states $|\alpha e^{i\pi/4}\rangle$, $|\alpha e^{-i\pi/4}\rangle$, $|\alpha e^{-i3\pi/4}\rangle$ and $|\alpha e^{i3\pi/4}\rangle$ in equation (8) are $(0, 2\sqrt{10})$, $(2\sqrt{10}, 0)$,

$(0, -2\sqrt{10})$, and $(-2\sqrt{10}, 0)$, respectively. Figure 1 shows the contour plot of Wigner function at $t = T_{\text{rev}}/4$, which clearly shows the superposition of four states at the locations mentioned above.

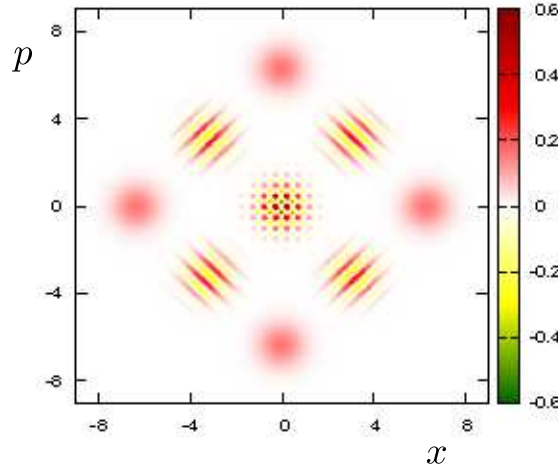


Figure 1. Contour plot of Wigner function at $T_{\text{rev}}/4$ for an initial coherent state $|\alpha\rangle$ with $\nu = |\alpha|^2 = 20$. It shows superposition of four coherent states $|\alpha e^{i\pi/4}\rangle$, $|\alpha e^{-i\pi/4}\rangle$, $|\alpha e^{-i3\pi/4}\rangle$ and $|\alpha e^{i3\pi/4}\rangle$ centered at $(0, 2\sqrt{10})$, $(2\sqrt{10}, 0)$, $(0, -2\sqrt{10})$, and $(-2\sqrt{10}, 0)$, respectively.

Next, we discuss the manifestations of fractional revivals in moments of observables. The time dependence of all moments of x and p can be obtained from the general result [8]

$$\begin{aligned}
 \langle a^{\dagger r} a^{r+s} \rangle &= \langle \psi(t) | a^{\dagger r} a^{r+s} | \psi(t) \rangle = \alpha^s \nu^r e^{-\nu(1 - \cos 2s\chi t)} \\
 &\times \exp[-i\chi(s(s-1) + 2rs)t - i\nu \sin 2s\chi t],
 \end{aligned} \tag{10}$$

where r and s are non-negative integers. The time dependence of k^{th} moment of x and p is strongly controlled by the factor $\exp[-\nu(1 - \cos 2k\chi t)]$, $k = 1, 2, \dots$, that modulates the oscillatory term. This acts as a strong damping factor for large values of ν , except when $\cos(2k\chi t)$ is near unity. This happens precisely at revivals (when $t = n\pi/\chi$, an integer multiples of T_{rev}) and at the fractional revival times $t = (n + j/k)T_{\text{rev}}$. Thus, by settings ν at a suitably large value, we ensure that the moments are essentially static, bursting into rapid variation at specific instants of time before reverting to quiescence. It can be concluded that k -sub-packet fractional revivals are captured in the k^{th} moment of x or p [8] but not in lower momets. In between $t = 0$ and $t = T_{\text{rev}}$, k^{th} moment of x or p captures the signature of $2, 3, \dots, k$ -sub-packet fractional revivals. For example, figure 2 shows the variation of $\langle x^4 \rangle$ versus t for an initial coherent state with $\nu = 100$. The dynamics of 4^{th} moment of x captures the signatures of four-sub-packet fractional

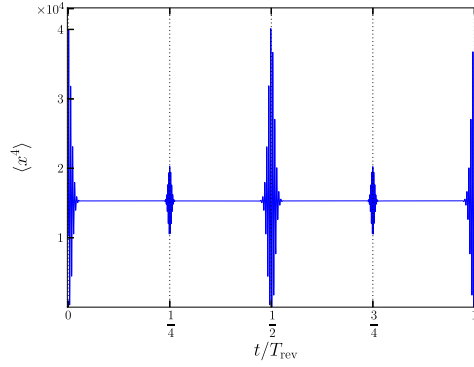


Figure 2. $\langle x^4(t) \rangle$ as a function of t/T_{rev} for an initial coherent state $|\alpha\rangle$ with $\nu = |\alpha|^2 = 100$. In between $t = 0$ and $t = T_{\text{rev}}$, $\langle x^4(t) \rangle$ is constant most of the time except at fractional revival times $t = j T_{\text{rev}}/4$, where $j = 1, 2, 3$. At these instants, 4th moment of x shows a rapid variation, which is a signature of 4 and 2-sub-packet fractional revivals.

revivals at $t/T_{\text{rev}} = 1/4$ and $3/4$ and the two-sub-packet fractional revival time at $t/T_{\text{rev}} = 1/2$ in between $t = 0$ and T_{rev} .

We also use Rényi entropy to analyze the fractional revival phenomena [10]. In terms of a generalized probability density $f(x)$ Rényi entropy is defined as [19]

$$R_f^{(\zeta)} \equiv \frac{1}{1-\zeta} \ln \int_{-\infty}^{\infty} [f(x)]^{\zeta} dx \quad \text{for } 0 < \zeta < \infty. \quad (11)$$

In terms of probability density in position and momentum spaces, $\rho(x) = |\psi(x)|^2$ and $\gamma(p) = |\phi(p)|^2$, respectively, the Rényi uncertainty relation is given by

$$R_{\rho}^{(\zeta)} + R_{\gamma}^{(\eta)} \geq -\frac{1}{2(1-\zeta)} \ln \frac{\zeta}{\pi} - \frac{1}{2(1-\eta)} \ln \frac{\eta}{\pi}, \quad (12)$$

with $1/\zeta + 1/\eta = 2$. As $\zeta \rightarrow 1$ and $\eta \rightarrow 1$ the Rényi uncertainty relations reduces to Shannon's, $S_{\rho} + S_{\gamma} \geq 1 + \ln(\pi)$. The entropy function takes local minima at fractional revival times and thus the signatures of fractional revivals are given by the local minima of $R_{\rho}^{(\zeta)}(t) + R_{\gamma}^{(\eta)}(t)$. Studies based on Rényi uncertainty relations for the fractional revivals of infinite square well and quantum bouncer have been reported in [20, 21]. Figure. 3 displays the time evolution of $R_{\rho}^{(2/3)} + R_{\gamma}^{(2)}$ versus t/T_{rev} for an initial coherent state in Kerr media. In this figure we have plotted up to $T_{\text{rev}}/2$ because it captures all important fractional revivals. The main fractional revivals are denoted by the vertical dotted lines in figure 3.

3. Evolution of two superposed coherent states

Consider the symmetric superposition of two coherent states (set $l = 2$ in equation (5))

$$|\psi_2\rangle = N_2 [|\alpha\rangle + |-\alpha\rangle], \quad (13)$$

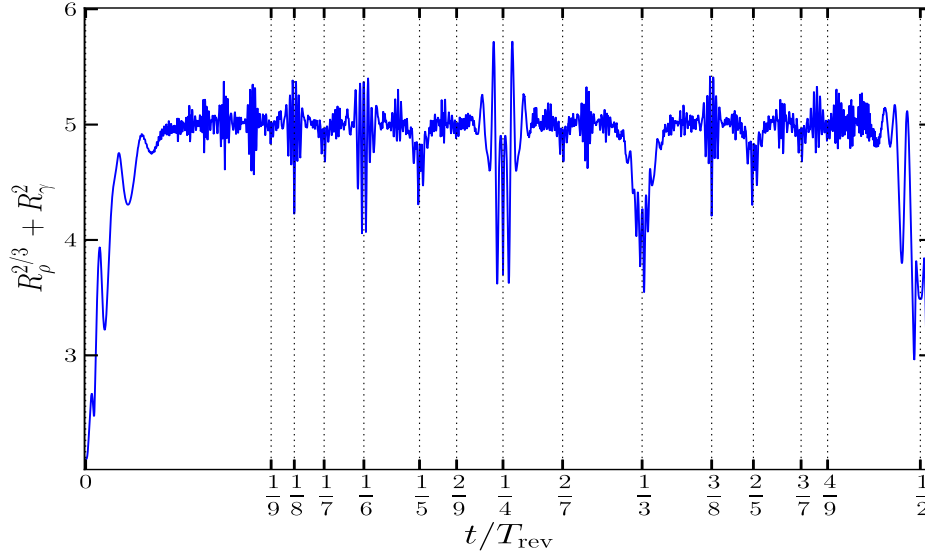


Figure 3. Time evolution of $R_\rho^{(2/3)} + R_\gamma^{(2)}$ for an initial coherent state with $\nu = |\alpha|^2 = 35$. The main fractional revivals are indicated by vertical dotted lines.

where the normalization constant

$$N_2 = \frac{1}{\sqrt{2}} [1 + \exp(-2|\alpha|^2)]^{-\frac{1}{2}}. \quad (14)$$

By setting $l = 2$ in equation (6) we obtain the Fock state representation of the even coherent state

$$|\psi_2\rangle = 2N_2 e^{-|\alpha|^2/2} \sum_{n=0}^{\infty} \frac{\alpha^{2n}}{\sqrt{(2n)!}} |2n\rangle. \quad (15)$$

Consider the dynamics of the initial state $|\psi_2\rangle$ governed by the nonlinear Hamiltonian given in equation (7). In between $t = 0$ and $t = T_{\text{rev}}$, at $t = jT_{\text{rev}}/4$, where $j = 1, 2$ and 3 , the state is again an even coherent state but rotated in phase space:

$$\begin{aligned} |\psi(T_{\text{rev}}/4)\rangle &= N_2 \left[|\alpha e^{-i\pi/4}\rangle + |-\alpha e^{-i\pi/4}\rangle \right] \\ |\psi(T_{\text{rev}}/2)\rangle &= N_2 \left[|\alpha e^{i\pi/2}\rangle + |-\alpha e^{i\pi/2}\rangle \right], \\ |\psi(3T_{\text{rev}}/4)\rangle &= N_2 \left[|\alpha e^{i\pi/4}\rangle + |-\alpha e^{i\pi/4}\rangle \right]. \end{aligned}$$

Figure 4 shows the plots of the Wigner function for the states $|\psi(0)\rangle = |\psi_2\rangle$ and $|\psi(T_{\text{rev}}/4)\rangle$. The unitary time evolution operator at $t = T_{\text{rev}}/4$ rotates the initial even coherent state 45 degree clockwise direction in phase space.

Here, k -sub-packet fractional revival occurs at time $t = jT_{\text{rev}}/4k$ where $j = 1, 2, \dots, (4k-1)$ for a given value of $k(> 1)$ with $(j, 4k) = 1$. At k -sub-packet fractional revival time the initial wave packet splits into k sub-packets. In contrast, we have seen earlier that for an initial coherent state k -sub-packet fractional revival occurs at

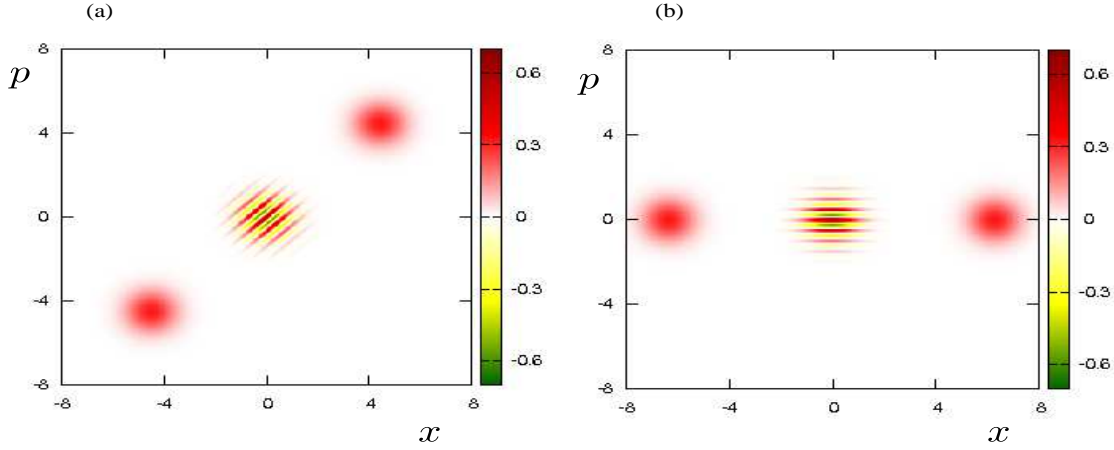


Figure 4. Contour plot of Wigner function at (a) $t = 0$ and (b) $t = T_{\text{rev}}/4$ for an initial even coherent state with $\nu = |\alpha|^2 = 20$. The unitary time evolution operator at $t = T_{\text{rev}}/4$ rotates the initial even coherent state 45 degree clockwise direction in phase space.

$t = jT_{\text{rev}}/k$, where $j = 1, 2, \dots, (k-1)$ for a given value of $k(> 1)$ with $(j, k) = 1$. For example, two sub-packet fractional revival for an initial even coherent state occurs at $t = T_{\text{rev}}/8$ and the state at this time is a superposition of two even coherent state,

$$\begin{aligned} |\psi(T_{\text{rev}}/8)\rangle &= C_1 N_2 \left[|\alpha e^{i\pi/8}\rangle + |-\alpha e^{i\pi/8}\rangle \right] \\ &+ C_2 N_2 \left[|\alpha e^{-i3\pi/8}\rangle + |-\alpha e^{-i3\pi/8}\rangle \right], \end{aligned} \quad (16)$$

where $C_1 = (1 - i)/2$ and $C_2 = (1 + i)/2$. Figure 5 clearly shows the superposition of two even coherent state at $t = T_{\text{rev}}/8$.

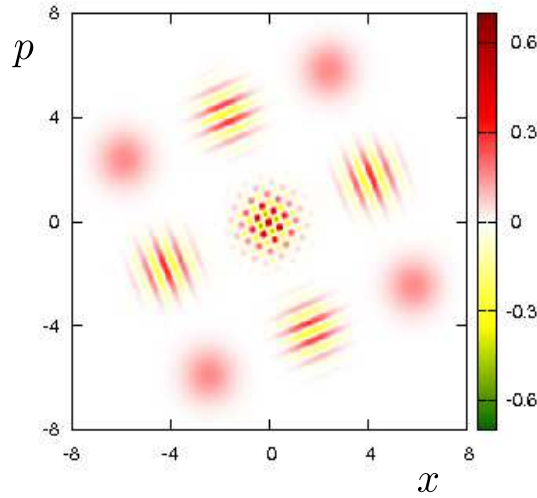


Figure 5. Contour plot of Wigner function at two-sub-packet fractional revival time $t = T_{\text{rev}}/8$ for an initial even coherent state with $\nu = |\alpha|^2 = 20$. It shows the superposition of two even coherent states (see equation (16)).

All odd moments of the operator x and p vanish at all times for the initial even coherent state. The expectation value of x^2 at any time can be obtained as explicit functions of t in the form

$$\begin{aligned} \langle x^2(t) \rangle = & 2N_2^2 \nu \left[e^{-\nu(1-\cos 4\chi t)} \cos \left(2\chi t + \nu \sin 4\chi t - \frac{\pi}{4} \right) \right. \\ & \left. + e^{-\nu(1+\cos(4\chi t))} \cos \left(2\chi t - \nu \sin(4\chi t) - \frac{\pi}{4} \right) \right] + \nu + \frac{1}{2} \end{aligned} \quad (17)$$

In between $t = 0$ and T_{rev} , the above expression for $\langle x^2 \rangle$ is static most of the time except at $t = T_{\text{rev}}/4, T_{\text{rev}}/2$ and $3T_{\text{rev}}/4$ for sufficiently large value of ν . Thus, the second moment of x^2 captures the signature of wave packet rotation in phase space at $T_{\text{rev}}/4, T_{\text{rev}}/2$ and $3T_{\text{rev}}/4$. Figure 6 shows the variation of the expectation value $\langle x^2 \rangle$ versus time for the initial even coherent state.

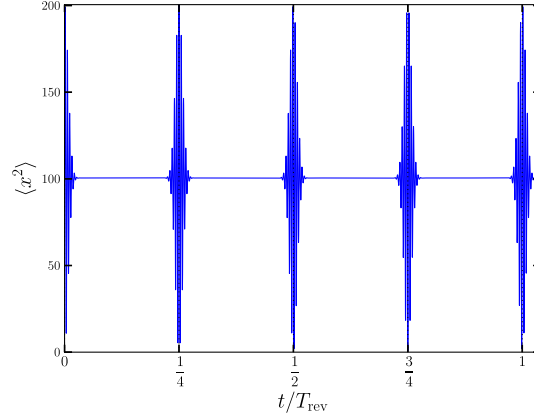


Figure 6. $\langle x^2(t) \rangle$ as a function of t/T_{rev} for an initial even coherent state $|\psi_2\rangle$ with $\nu = |\alpha|^2 = 100$. In between $t = 0$ and T_{rev} , the second moment of x is constant most of the time except at $T_{\text{rev}}/4, T_{\text{rev}}/2$ and $3T_{\text{rev}}/4$. At these instants, 2nd moment of x shows a rapid variation, which is a signature of wave packet rotation.

Expressions for the $2k^{\text{th}}$ moments of x and p can be deduced readily from the general result

$$\begin{aligned} \langle a^{2k} \rangle = & 2N_2^2 \alpha^{2k} \left\{ e^{-\nu(1-\cos 4k\chi t)} \exp[-2ik(2k-1)\chi t - i\nu \sin 4k\chi t] \right. \\ & \left. + e^{-\nu(1+\cos 4k\chi t)} \exp[-2ik(2k-1)\chi t + i\nu \sin 4k\chi t] \right\}, \end{aligned} \quad (18)$$

where k is a positive integer. The time dependence of $2k^{\text{th}}$ moments of x is strongly controlled by the factors $\exp[-\nu(1 \pm \cos 4k\chi t)]$, $k = 1, 2, \dots$, that modulates the oscillatory term. In between $t = 0$ and $t = T_{\text{rev}}$, these factors act as a strong damping factor for large values of ν , except at fractional revival times $t = jT_{\text{rev}}/4k$. It can be concluded that k -sub-packet fractional revivals are captured in the $2k^{\text{th}}$ moment of x or p but not in lower moments. These results are illustrated in figures 7 (a) and 7 (b). Figure 7 (a) shows the temporal evolution of the expectation value $\langle x^4(t) \rangle$. It shows rapid oscillations at $t/T_{\text{rev}} = j/8$, where $j = 1, 2, \dots, 7$ in between $t = 0$ and T_{rev} . Thus,

the fourth moment of x versus time captures the signature of 2-sub-packet fractional revivals at $t/T_{\text{rev}} = j/8$ where $j = 1, 2, \dots, 7$ with $(j, 8) = 1$ and wave packet rotations at $t/T_{\text{rev}} = j/4$ where $j = 1, 2, 3$. Figure 7 (b) is a plot of $\langle x^6(t) \rangle$ versus time which shows the signature of 3 sub-packet fractional revival.

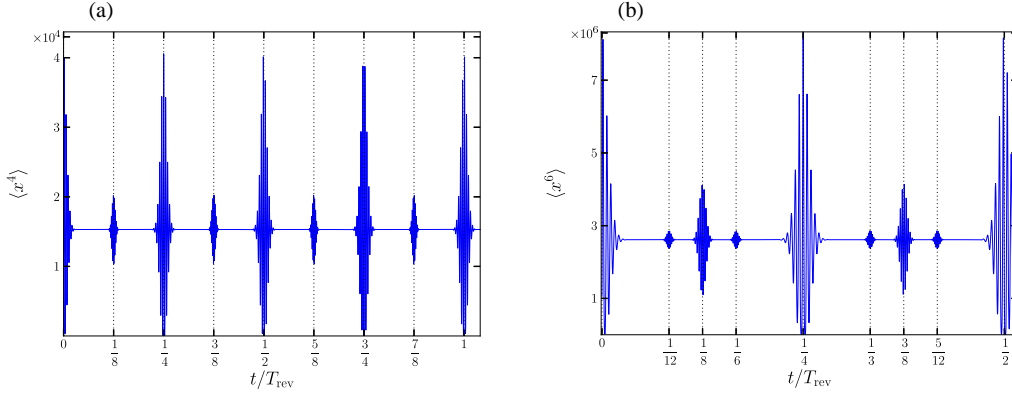


Figure 7. Temporal evolution of higher moments of x for an initial even coherent state $|\psi_2\rangle$ with $\nu = |\alpha|^2 = 100$. (a) In between $t = 0$ and $t = T_{\text{rev}}$, $\langle x^4(t) \rangle$ is constant most of the time except at $t = j T_{\text{rev}}/8$, where $j = 1, 2, \dots, 7$. At these instants, 4th moment of x shows a rapid variation, which is the signature of two-sub-packet fractional revival and wave packet rotation. (b) In this figure we have plotted between $t = 0$ and $T_{\text{rev}}/2$ for a better view. $\langle x^6(t) \rangle$ is constant most of the time except at $t = j T_{\text{rev}}/12$, where $j = 1, 2, \dots, 6$. At these instants, 6th moment of x shows a rapid variation, which is the signature of three and two-sub-packet fractional revivals and wave packet rotation.

We also studied the temporal evolution of Rényi uncertainty relation for the initial even coherent state. Figure 8 shows the Rényi uncertainty versus time for the initial even coherent state with $\nu = 30$. Signatures of fractional revivals are indicated by the local minima of Rényi uncertainty. Our analysis shows the clear distinction between time evolution of initial state of the form $\sum_n C_n |n\rangle$ and $\sum_n C_n |2n\rangle$. In the next section we study the dynamics of an initial state which is of the form $\sum_n C_n |3n\rangle$.

4. Evolution of the initial state of the form $\sum C_n |3n\rangle$

Setting $l = 3$ in equation (5), we get superposition of three coherent states

$$|\psi_3\rangle = N_3 \left[|\alpha\rangle + |\alpha e^{i2\pi/3}\rangle + |\alpha e^{-i2\pi/3}\rangle \right], \quad (19)$$

which in Fock space is given by

$$|\psi_3\rangle = 3N_3 e^{-|\alpha|^2/2} \sum_{n=0}^{\infty} \frac{\alpha^{3n}}{\sqrt{3n!}} |3n\rangle. \quad (20)$$

Time evolution of the initial state $|\psi_3\rangle$ shows fractional revivals and rotations at different instants when compared to the initial coherent state and the initial even coherent state. For the initial state $|\psi_3\rangle$, the rotations in phase space occur at $t = j T_{\text{rev}}/9$, where $j = 1, 2, \dots, 8$ in between $t = 0$ and $t = T_{\text{rev}}$. In the case of

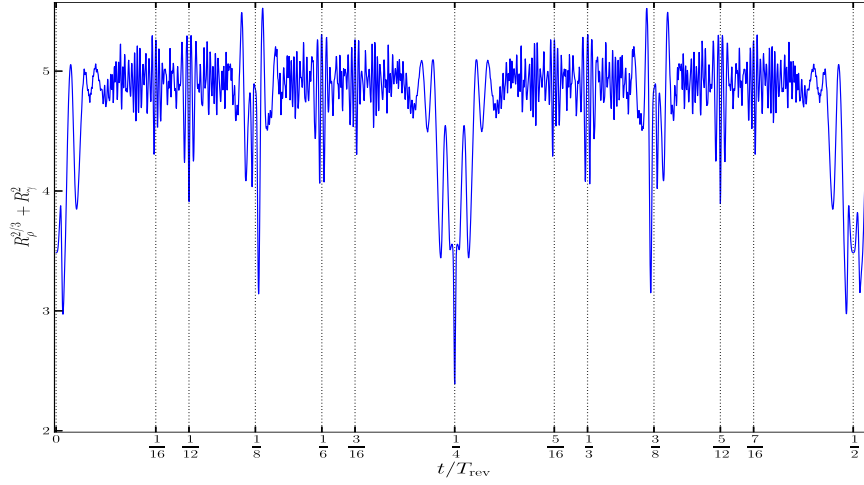


Figure 8. Time evolution of $R_p^{(2/3)} + R_\gamma^{(2)}$ for an initial even coherent state with $\nu = 30$. The main fractional revivals are indicated by vertical dotted lines.

initial coherent state there is no rotation and for an initial even coherent state rotations occur at $t = jT_{\text{rev}}/4$, where $j = 1, 2$, and 3 . For example at $t = T_{\text{rev}}/9$, the initial state $|\psi_3\rangle$ evolves to

$$|\psi(T_{\text{rev}}/9)\rangle = N_3 \left[|\alpha e^{-i8\pi/9}\rangle + |\alpha e^{-i2\pi/9}\rangle + |\alpha e^{i4\pi/9}\rangle \right].$$

Figure 9 shows the plots of the Wigner function for the states $|\psi(0)\rangle = |\psi_3\rangle$ and $|\psi(T_{\text{rev}}/9)\rangle$. The unitary time evolution operator at $t = T_{\text{rev}}/9$ rotates the initial state 45 degree clockwise direction in the phase space.

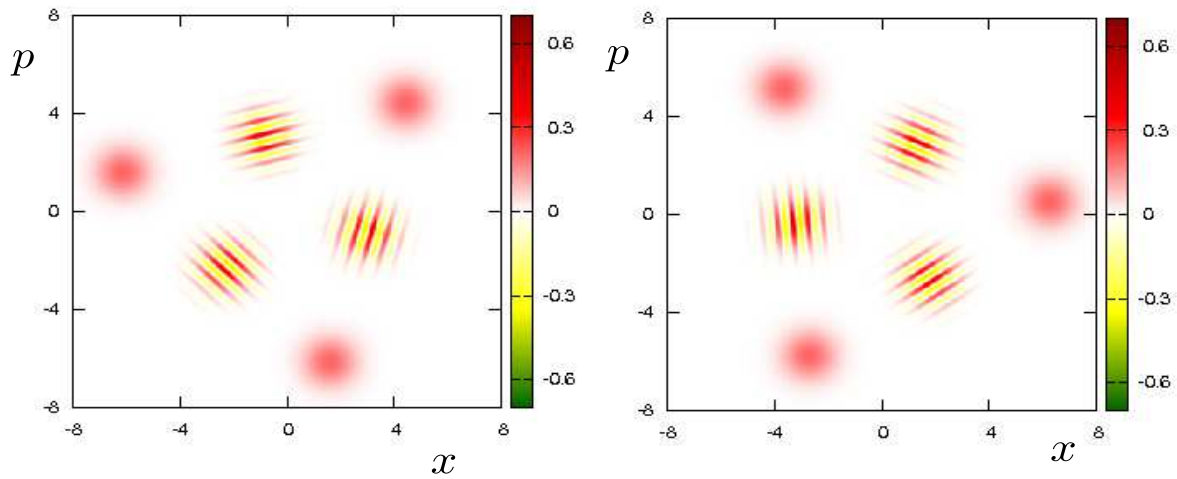


Figure 9. Contour plot of Wigner function at $t = 0$ (left) and $t = T_{\text{rev}}/9$ (right) for the initial state $|\psi_3\rangle$ with $\nu = |\alpha|^2 = 20$. Both the figures show superposition of three coherent states. The unitary time evolution operator at $t = T_{\text{rev}}/9$ rotates the initial state 45 degree clockwise direction in the phase space.

Here, k -sub-packet fractional revival occurs at time $t = jT_{\text{rev}}/9k$ where $j =$

$1, 2, \dots, (9k - 1)$ for a given value of $k(> 1)$ with $(j, 9k) = 1$. For example, two sub-packet fractional revival for an initial state occurs at $t = T_{\text{rev}}/18$ and the state at this time is a superposition of two states of the form $|\psi_3\rangle$:

$$|\psi(T_{\text{rev}}/18)\rangle = C_1 N_3 [\alpha e^{-i11\pi/18}\rangle + \alpha e^{i\pi/18}\rangle + \alpha e^{i13\pi/18}\rangle] \\ + C_2 N_3 [\alpha e^{-i17\pi/18}\rangle + \alpha e^{-i5\pi/8}\rangle + \alpha e^{i7\pi/18}\rangle], \quad (21)$$

where $C_1 = (1 - i)/2$ and $C_2 = (1 + i)/2$. Figure 10 clearly shows the superposition of two initial states given in equation (19) with different α values as given in equation (21) at $t = T_{\text{rev}}/18$.

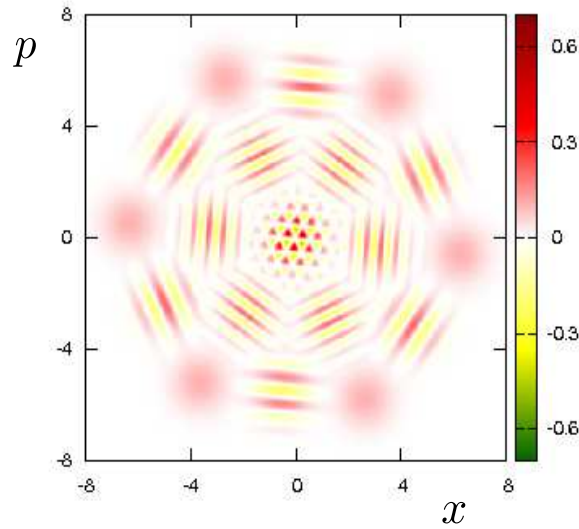


Figure 10. Contour plot of Wigner function at $t = T_{\text{rev}}/18$ for the initial state $|\psi_3\rangle$ with $\nu = |\alpha|^2 = 20$. It shows the superposition of two states in the form of $|\psi_3\rangle$.

Only the $3k^{\text{th}}$ (where $k = 1, 2, \dots$) moment of x and p gives non-zero value and all other moments are identically equal to zero at all times for the initial state $|\psi_3\rangle$. The expectation value of x^3 at any time for an initial state $|\psi_3\rangle$ is

$$\langle x^3(t) \rangle = 3N_3^2 \nu^{3/2} [e^{-\nu(1-\cos 6\chi t)} \cos(6\chi t + \nu \sin 6\chi t - 3\pi/4) \\ + e^{-\nu(1-\sin(6\chi t - \pi/6))} \cos(6\chi t + \nu \cos(6\chi t + \pi/6) - 3\pi/4) \\ + e^{-\nu(1+\sin(6\chi t + \pi/6))} \cos(6\chi t - \nu \cos(6\chi t - \pi/6) - 3\pi/4)] \quad (22)$$

In between $t = 0$ and T_{rev} , the above expression for $\langle x^3 \rangle$ is zero most of the times except at $t = jT_{\text{rev}}/9$, where $j = 1, 2, \dots, 8$ for sufficiently large value of ν . These instants correspond to wave packet rotation in phase space. Figure 11 shows the variation of the expectation value $\langle x^3 \rangle$ versus time for the initial state $|\psi_3\rangle$. It shows that wave packet rotation in phase space is captured in the third moment of x . Expressions for the higher moments of x and p can be deduced readily from the general result

$$\langle a^{3k} \rangle = 3N_3^2 \alpha^{3k} \left\{ e^{-\nu(1-\cos 6k\chi t)} \exp[-3ik(3k-1)\chi t - i\nu \sin 6k\chi t] \right. \\ \left. + e^{-\nu(1-\sin(6k\chi t - \pi/6))} \exp[-3ik(3k-1)\chi t - i\nu \cos(6k\chi t + \pi/6)] \right.$$

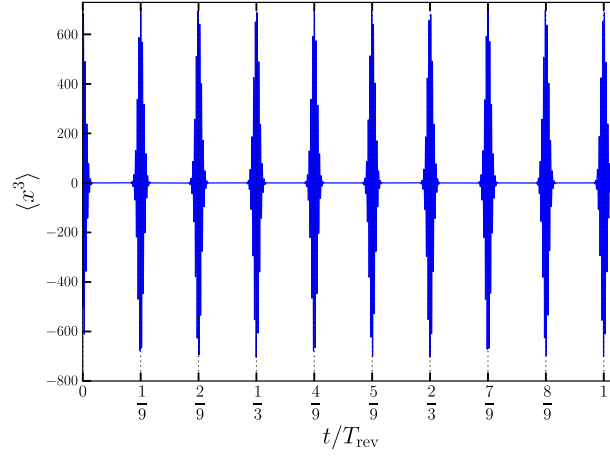


Figure 11. $\langle x^3(t) \rangle$ as a function of t/T_{rev} for the initial state $|\psi_3\rangle$ with $\nu = |\alpha|^2 = 100$. In between $t = 0$ and T_{rev} , the third moment of x is constant most of the time except at $t = jT_{\text{rev}}/9$ where $j = 1, 2, \dots, 8$. At these instants of time the evolved state is a rotated initial wave packet.

$$+ e^{-\nu(1+\sin(6k\chi t+\pi/6))} \exp[-3ik(3k-1)\chi t + i\nu \cos(6k\chi t - \pi/6)] \} \quad (23)$$

The time dependence of $3k^{\text{th}}$ moments of x is strongly controlled by the factors $\exp[-\nu(1 - \cos 6k\chi t)]$ and $\exp[-\nu(1 \pm \sin(6k\chi t - \pi/6))]$, $k = 1, 2, \dots$, that modulates the oscillatory term. In between $t = 0$ and $t = T_{\text{rev}}$, these factors act as a strong damping factor for large values of ν , except at fractional revival times $t = jT_{\text{rev}}/9k$. It can be concluded that k -sub-packet fractional revivals are captured in the $3k^{\text{th}}$ moment of x or p . These results are illustrated in figures 12 (a) and 12 (b). Figure 12 (a) shows the temporal evolution of the expectation value $\langle x^6(t) \rangle$. We have plotted the graph in between $t = 0$ and $T_{\text{rev}}/2$ for a better view. It confirms that sixth moment of x captures the signature of 2-sub-packet fractional revival and rotations. Figure 12 (b) is a plot of $\langle x^9(t) \rangle$ versus time which shows the signature of 3-sub-packet fractional revivals and rotations. Figure 13 shows the Rényi uncertainty versus time for the initial state $|\psi_3\rangle$ with $\nu = 30$. Again, it confirms our analysis based on the expectation values. The main fractional revivals are indicated by vertical dotted lines in the figure. So far we have studied the dynamics of initial states of the form $\sum_n C_n |ln\rangle$, where $l = 1, 2$ and 3. In the next section we generalize our results for a general l .

5. Summary

We have extended the analysis carried out in the above sections for an initial wave packet $|\psi_l\rangle$ given in equation (5) for a general l . For ready reference, we write it down

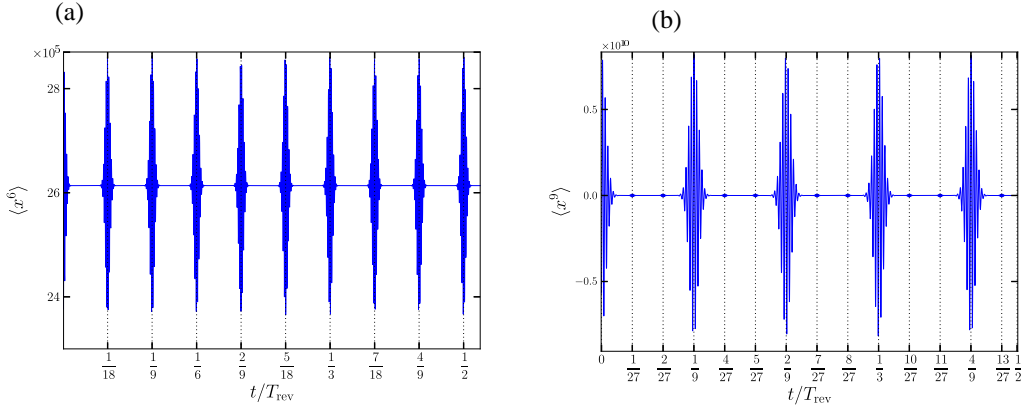


Figure 12. Temporal evolution of higher moments of x for an initial state $|\psi_3\rangle$ with $\nu = |\alpha|^2 = 100$. (a) $\langle x^6(t) \rangle$ is constant most of the time except at $t = j T_{\text{rev}}/18$, where $j = 1, 2, \dots, 9$. At these instants, 6th moment of x shows a rapid variation, which is a signature of two-sub-packet fractional revival and wave packet rotation. (b) $\langle x^9(t) \rangle$ is constant most of the time except at $t = j T_{\text{rev}}/27$, where $j = 1, 2, \dots, 13$. At these instants, 9th moment of x shows a rapid variation, which is a signature of three-sub-packet fractional revival and wave packet rotation.

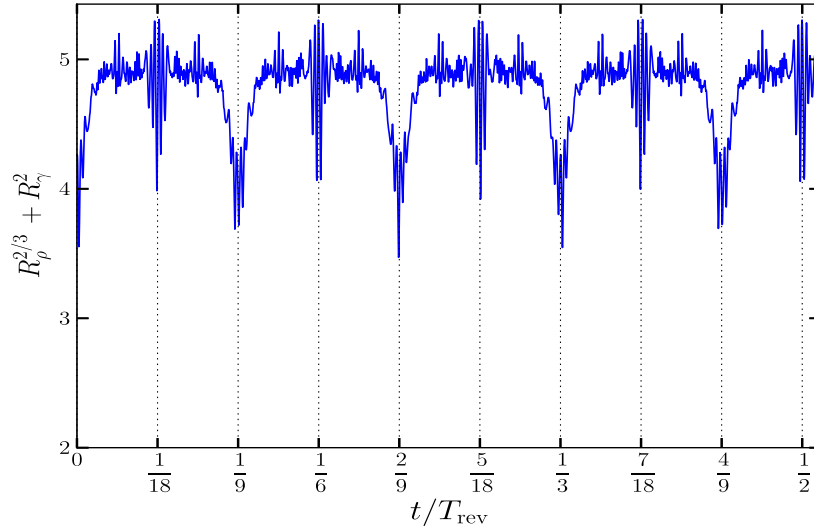


Figure 13. Time evolution of $R_\rho^{(2/3)} + R_\gamma^{(2)}$ for the initial state $|\psi_3\rangle$ with $\nu = 30$. The main fractional revivals are indicated by vertical dotted lines.

again the Fock state representation of $|\psi_l\rangle$:

$$|\psi_l\rangle = l N_l e^{-\nu/2} \sum_{n=0}^{\infty} \frac{\alpha^{ln}}{\sqrt{(ln)!}} |ln\rangle. \quad (24)$$

We investigated the dynamics of initial state $|\psi_l\rangle$ with $l > 3$ and found the following general results:

- (i) The time evolved state at $t = j T_{\text{rev}}/l^2$, where $j = 1, 2, \dots, (l^2 - 1)$, is a rotated

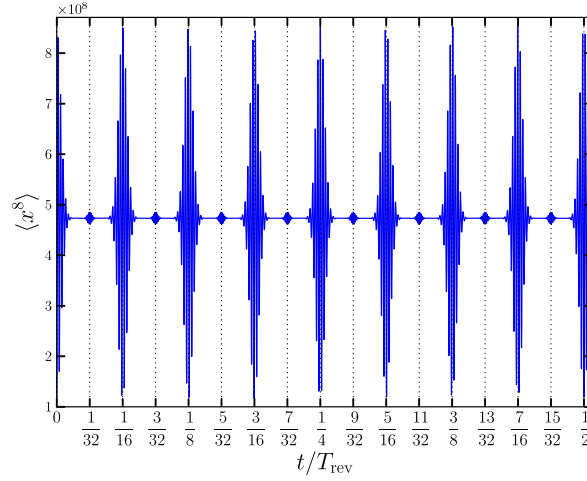


Figure 14. $\langle x^8(t) \rangle$ as a function of t/T_{rev} for the initial state $|\psi_4\rangle$ with $\nu = |\alpha|^2 = 100$. In between $t = 0$ and $t = T_{\text{rev}}/2$, $\langle x^8(t) \rangle$ is constant most of the time except at $t = j T_{\text{rev}}/32$, where $j = 1, 2, \dots, 16$. At these instants, 8th moment of x shows a rapid variation, which is a signature of two-sub-packet fractional revival and wave packet rotation.

initial wave packet.

- (ii) k -sub-packet fractional revival occur at $t = j T_{\text{rev}}/l^2 k$ where $j = 1, 2, \dots, (l^2 k - 1)$ for a given value of $k(> 1)$ with $(j, l^2 k) = 1$.
- (iii) The distinctive signatures of k sub-packet fractional revivals are captured in $(lk)^{\text{th}}$ moments of the operators x and p .

We do not write it down the analysis for higher values of l because it is repetitive, but for completeness we discuss the dynamics of an initial state $|\psi_4\rangle$. This initial state can be written as a superposition of 4 coherent states (see equation (5)). According to the result (ii) quoted above, two-sub-packet fractional revival of the initial state $|\psi_4\rangle$ occur at $t = T_{\text{rev}}/32$. Indeed the initial state $|\psi_4\rangle$ shows two-sub-packet fractional revival at $t = T_{\text{rev}}/32$:

$$|\psi(T_{\text{rev}}/32)\rangle = N_4 C_1 \left[|\alpha e^{-i31\pi/32}\rangle + |\alpha e^{-i15\pi/32}\rangle + |\alpha e^{i\pi/32}\rangle + |\alpha e^{i17\pi/32}\rangle \right] \\ + N_4 C_2 \left[|\alpha e^{-i23\pi/32}\rangle + |\alpha e^{-i7\pi/32}\rangle + |\alpha e^{i9\pi/32}\rangle + |\alpha e^{i25\pi/32}\rangle \right],$$

where $C_1 = (1-i)/2$ and $C_2 = (1+i)/2$. For the same initial state $|\psi_4\rangle$, Figure 14 shows the temporal evolution of the expectation value $\langle x^8(t) \rangle$. We have plotted till $t = T_{\text{rev}}/2$ for a better view, i.e., j runs only up to 16 instead of 31 in the result (ii). It captures the signature of 2-sub-packet fractional revival at $t = j T_{\text{rev}}/32$ where $j = 1, 2, \dots, 16$ with $(j, 32) = 1$ and wave packet rotations at $t = j T_{\text{rev}}/16$, where $j = 1, 2, \dots, 8$, which confirms our general result (iii) quoted above.

Experimental manifestations of our results are possible using continuous-variable quantum-state tomography. The moments of the operators x and p can be

experimentally measured using homodyne correlation techniques with a weak local oscillator [22]. Wigner function have been reconstructed from the measurements of the quantum statistics of the quadrature operator x [23,24]. Recently, the experimental characterization of photon creation and annihilation operators has been reported [25]. It may possible to measure the Rényi entropy using the techniques described in [26,27].

Acknowledgments

The authors would like to sincerely thank the anonymous reviewers for their valuable comments and suggestions.

References

- [1] R.W. Robinett 2004 *Phys. Rep.* **392** 1
- [2] I.Sh. Averbukh, N.F. Perelman 1989 *Phys. Lett. A* **139** 449
- [3] J. A. Yeazell, C.R. Stroud Jr. 1991 *Phys. Rev. A* **43** 5153
- [4] M. J. J. Vrakking, D. M. Villeneuve, A. Stolow 1996 *Phys. Rev. A* **54** R37
- [5] M. Greiner, O. Mandel, T. W. Hänsch, I. Bloch 2002 *Nature* **419** 51
- [6] M. Leibscher and I. Sh. Averbukh 2001 *Phys. Rev. A* **63** 043407
- [7] Uwe R. Fischer, Bo Xiong 2011 *Phys. Rev. A* **84** 063635
- [8] C. Sudheesh, S. Lakshmibala, V. Balakrishnan 2004 *Phys. Lett. A* **329** 14
- [9] J. A. Vaccaro, A. Orłowski 1995 *Phys. Rev. A* **51** 4172
- [10] E. Romera, F. de los Santos 2007 *Phys. Rev. Lett.* **99** 263601
- [11] G.J. Milburn 1986 *Phys. Rev. A* **33** 674
- [12] M. Kitagawa, Y. Yamamoto 1986 *Phys. Rev. A* **34** 3974
- [13] K. Tara, G.S. Agarwal, S. Chaturvedi 1993 *Phys. Rev. A* **47** 5024
- [14] A. Miranowicz, R. Tanaś, S. Kielich 1990 *Quantum Opt.* **2** 253
- [15] B. Yurke, D. Stoler 1986 *Phys. Rev. Lett.* **57** 13
- [16] G. S. Agarwal, K. Tara 1991 *Phys. Rev. A* **43** 492
- [17] C. Sudheesh, S. Lakshmibala, V. Balakrishnan 2005 *Europhys. Lett.* **71** 744
- [18] A. Napoli, A. Messina 1999 *Eur. Phys. J. D* **5** 441
- [19] I. Bialynicki-Birula 2006 *Phys. Rev. A* **74** 052101
- [20] E. Romera, F. de los Santos 2008 *Phys. Rev. A* **78** 013837
- [21] F. de los Santos, Clara Guglieri, E. Romera 2010 *Physica E* **42** 303
- [22] E. V. Shchukin, W. Vogel 2005 *Phys. Rev. A* **72** 043808
- [23] G. Breitenbach, S. Schiller, J. Mlynek 1997 *Nature* **387** 471
- [24] A. I. Lvovsky, M. G. Raymer 2009 *Rev. Mod. Phys.* **81** 299
- [25] R. Kumar, E. Barrios, C. Kupchak, A. I. Lvovsky 2013 *Phys. Rev. Lett.* **110** 130403
- [26] A. J. Daley, H. Pichler, J. Schachenmayer, P. Zoller 2012 *Phys. Rev. Lett.* **109** 020505
- [27] Dmitry A. Abanin, Eugene Demler 2012 *Phys. Rev. Lett.* **109** 020504